Two-atom dark states in electromagnetic cavities

G. J. Yang,* O. Zobay, and P. Meystre

Optical Sciences Center, University of Arizona, Tucson, Arizona 85721
(Received 14 November 1998)

The center-of-mass motion of two two-level atoms coupled to a single damped mode of an electromagnetic resonator is investigated. For the case of one atom being initially excited and the cavity mode in the vacuum state, it is shown that the atomic time evolution is dominated by the appearance of dark states. These states, in which the initial excitation is stored in the internal atomic degrees of freedom and the atoms become quantum mechanically entangled, are almost immune against photon loss from the cavity. Various properties of the dark states within and beyond the Raman-Nath approximation of atom optics are worked out.
[S1050-2947(99)06105-3]

PACS number(s): 42.50.Ct, 42.50.Fx, 42.50.Vk

I. INTRODUCTION

Recent advances in cavity quantum electrodynamics have significantly expanded our understanding of the interaction between matter and the quantized electromagnetic field [1,2]. A central topic in these studies is the theoretical and experimental investigation of situations in which a single atom interacts with a small number of modes of the radiation field in high-Q optical or microwave resonators. In such a setting, the dynamical behavior of the atom is evidently very different from the free-space situation and one can observe phenomena such as inhibited and enhanced spontaneous emission [3,4] or Rabi oscillations between two electromagnetically coupled states [5]. A natural extension of these studies concerns the modification of the interaction between two atoms in a cavity environment. As the interatomic interaction is ultimately mediated by the electromagnetic field, one can expect drastic effects also in this case. The interest in this problem has recently grown, stimulated in part by the remarkable experiments of Refs. [6] and [7]. For example, several recent articles have examined the mutual coherence of the two atomic dipoles under various circumstances [8–11].

In a further study the modification of the near-resonant dipole-dipole interaction between two atoms confined to a cavity was investigated in detail [12]. As a main result it was shown that the familiar concept of the dipole-dipole potential ceases to be meaningful under certain circumstances. The purpose of the present paper is to continue and extend this work, the emphasis now being put on the investigation of the actual dynamical behavior of the atoms. In particular, we examine the atomic center-of-mass motion under the influence of their interaction with the cavity field. In order to work out basic aspects of the problem, we concentrate here on the model of a short and closed optical resonator in which the atoms interact exclusively with a single damped standing-wave mode of the electromagnetic radiation field. An initially excited atom will then spontaneously emit a photon into the cavity mode and subsequently reabsorb it. Con-

sequently, it experiences a random walk in momentum space, i.e., heating. Due to photon exchange the atom can also interact with and excite its partner in the cavity. These processes will cease, of course, as soon as the photon escapes the resonator due to cavity losses.

The analysis of this problem shows that, contrary to what one might expect intuitively, the presence of the second atom does not simply lead to some quantitative modifications in the heating and decay process of the first. Rather, it causes qualitative changes in the dynamical behavior of the system. In particular, one observes a tendency of the system to settle into so-called ''dark'' or ''quasidark'' states. These dark states consist of superpositions of states in which the initial excitation is stored in either atom 1 or atom 2, i.e., entangled states of the atoms-cavity system. Due to destructive quantum interferences, these superpositions are completely—or to a large degree—dynamically decoupled from the states in which the photon is present in the cavity. Thus they are immune—or almost immune—to photon decay. Atoms in these dark states can be thought of as a new kind of ''molecule'' largely delocalized and bound by the cavity electromagnetic field. The focus of the present paper is on an analysis of these dark states, which can be viewed as a generalization of the antisymmetric Dicke state of the theory of superradiance and subradiance [13]. To our knowledge, the persistence of the entangled two-atom dark states under the influence of the atomic center-of-mass motion has not been previously discussed in the literature.

Section II introduces our model and establishes the notation. In order to motivate the subsequent analysis, Sec. III discusses some numerical examples that illustrate the role of the dark states and demonstrate their long-livedness, even in the case of only approximate darkness. Section IV gives a detailed analytical discussion of the dark states. We first consider the dynamics of the atomic system in the Raman-Nath approximation (RNA), where the atoms are treated as infinitely massive. This allows for a very simple and transparent description of the effect. We then remove this approximation and demonstrate that certain RNA dark states do remain dark in the exact analysis. The decay rates of the other RNA dark states are estimated, and the analytical results compared to numerical calculations. A central result is that even though these states are only approximately dark, they still have ex-

---

*Permanent address: Department of Physics, Beijing Normal University, Beijing 100875, China.

tremely long lifetimes. This should render the existence of the quasidark states amenable to experimental observation, at least in principle. Finally, further remarks and conclusions are given in Sec. V.

II. MODEL

Our objective consists in studying the center-of-mass motion of two atoms confined by a trapping potential and interacting with the electromagnetic field inside a high-Q cavity. In order to work out most clearly some of the basic physical effects observable in this system, we investigate in the following an idealized model problem. Questions of experimental realizability will be discussed in Sec. V.

We consider the one-dimensional motion of two two-level atoms of mass M trapped inside an infinite square-well potential $V(x)$ with boundaries at $x=0$ and $x=L$. The upper and lower internal atomic states $|e\rangle$ and $|g\rangle$ are separated in energy by an amount of $\hbar\omega_0$. The atoms which are treated as distinguishable are also placed inside a short and closed electromagnetic cavity that is aligned with the atomic trap along the x axis. We assume the cavity characteristics to be such that the atomic interaction with the cavity field can be described as a coupling to a single mode. In particular, spontaneous photon emission into directions other than the x axis is disregarded. On the other hand, the damping of the relevant cavity mode due to its coupling to the electromagnetic vacuum outside the resonator is taken into account. Based on this description, the Hamiltonian of the system is

$$H = H_a + H_c + H_r + H_{ca} + H_{cr}, \qquad (1)$$

where H_a, H_c, and H_r are the free Hamiltonians of the atoms, the cavity mode, and the vacuum modes, respectively. They are given by

$$H_a = \sum_{j=1}^{2} \left(\frac{\hat{p}_j^2}{2M} + V(\hat{x}_j) + \hbar\omega_0 \sigma_j^\dagger \sigma_j \right), \qquad (2)$$

$$H_c = \hbar\omega_c a_c^\dagger a_c, \qquad H_r = \sum_\mu \hbar\omega_\mu a_\mu^\dagger a_\mu. \qquad (3)$$

Here, $\hat{p}_j$ is the center-of-mass momentum and $\hat{x}_j$ the position of the jth atom along the x axis. The atomic pseudospin operators σ_j are defined by $\sigma_j = |g,j\rangle\langle e,j|$. The annihilation operators for the cavity mode and the vacuum modes are denoted a_c and a_μ, respectively, and the mode frequencies are ω_c and ω_μ. The interaction of the cavity mode with the atoms and with the vacuum modes is described by the terms H_{ca} and H_{cr}. In the dipole and the rotating-wave approximation, they read

$$H_{ca} = \sum_{j=1}^{2} \hbar g \cos(kx_j + \phi)(\sigma_j^\dagger a_c + \sigma_j a_c^\dagger), \qquad (4)$$

$$H_{cr} = \sum_\mu \hbar(g_\mu^* a_c^\dagger a_\mu + g_\mu a_c a_\mu^\dagger), \qquad (5)$$

where $g = (\hbar\omega_c/2\varepsilon_0 L_c)^{1/2}$ denotes the atom-cavity coupling constant with L_c the cavity length. For a planar cavity the mode profile is cosine-shaped with wave vector k. The phase

angle ϕ characterizes the relative positioning between cavity mode and atomic trap. The coupling constant between the cavity mode and the μth vacuum mode is denoted g_μ.

In discussing the atomic time evolution, we will mostly be concerned with situations in which the center-of-mass wave function is spread out over a region of extension Δx large in comparison to the cavity mode wavelength $2\pi/k$ but small in comparison to the trap length L. For small enough times the existence of the trap walls may thus be neglected. Furthermore, it is assumed that the initial wave function can be ascribed a well-defined momentum (p_{01}, p_{02}) and that the effects of the (small) momentum spread around this initial value may be disregarded. From the form (4) of the atom-field coupling it follows that a single-atom state with momentum p is only coupled to states with momenta $p \pm \hbar k$. In view of our initial condition, we thus introduce the notation $|(i_1, m_1),(i_2, m_2), n_c, \{n_\mu\}\rangle$ that denotes a state where atom j has internal state i_j and momentum $q_{0j} + m_j \hbar k$ with integer m_j. Thereby, $q_{0j} = \mathrm{mod}(p_{0j}, \hbar k)$, i.e., $0 \le q_{0j} < \hbar k$. The number of photons in the cavity and the vacuum mode "μ" are denoted n_c and n_μ, respectively.

In case only one excitation is present in the system and within the realm of validity of the above approximations, the general expression for the system state vector is thus given by

$$\begin{aligned}
|\Psi(t)\rangle = \sum_{m,n} \Big\{ &C_{1,m,n}(t)|(e,m),(g,n),0,\{0_\mu\}\rangle \\
&+ C_{2,m,n}(t)|(g,m),(e,n),0,\{0_\mu\}\rangle \\
&+ C_{3,m,n}(t)|(g,m),(g,n),1,\{0_\mu\}\rangle \\
&+ \sum_\mu C_{4,m,n,\mu}(t)|(g,m),(g,n),0,\{1_\mu\}\rangle \Big\}. \quad (6)
\end{aligned}$$

We now proceed to eliminate the reservoir degrees of freedom in the system equations of motion with the help of the Born-Markov approximation. This introduces an exponential decay rate $\kappa/2 = \pi|g_\mu|^2$ and a frequency shift Δ_c in the dynamics of the amplitudes $C_{3,m,n}$. For the following, we incorporate this shift into the detuning Δ between the atomic resonance and the cavity frequency and work in the interaction picture with respect to ω_0. The effective Hamiltonian time evolution of the system before the photon escapes the cavity is then determined by

$$i\dot{C}_{1,m,n} = \omega_{m,n} C_{1,m,n} + \frac{g}{2}(C_{3,m+1,n} + C_{3,m-1,n}), \qquad (7)$$

$$i\dot{C}_{2,m,n} = \omega_{m,n} C_{2,m,n} + \frac{g}{2}(C_{3,m,n+1} + C_{3,m,n-1}), \qquad (8)$$

$$i\dot{C}_{3,m,n} = (\omega_{m,n} + \Delta - i\kappa/2)C_{3,m,n} + \frac{g}{2}(C_{1,m+1,n}$$
$$+ C_{1,m-1,n} + C_{2,m,n+1} + C_{2,m,n-1}) \qquad (9)$$

with

$$\omega_{m,n} = [(q_{01} + m\hbar k)^2 + (q_{02} + n\hbar k)^2]/(2\hbar M) \qquad (10)$$

describing the influence of kinetic energy. From Eqs. (7)–(9) one notices a further selection rule. For example, the set of coefficients $C_{1,m,n}$, with m,n both even, are only coupled among each other and to $C_{2,m',n'}$, m',n' odd and $C_{3,m'',n''}$, m'' odd, n'' even. Note also that Eqs. (7)–(9) can be written independently of the phase angle ϕ. In the following we set $\Delta=0$ for convenience.

Another interesting situation arises if one takes the existence of the atomic trap boundaries fully into account. In this case it is convenient to expand the center-of-mass wave functions in terms of the eigenfunctions of the atomic Hamiltonian (2), i.e., $2\sin(\pi q x_1/L)\sin(\pi r x_2/L)/L$, $q,r \geq 1$, which can be thought of as specific superpositions of momentum states with opposite wave vectors. In general, the coupling term H_{ac} introduces transitions from a single-particle eigenstate $\psi_q^{g(e)}=\sqrt{2/L}\sin(\pi q x_1/L)|g(e)\rangle$ to an infinite number of other states $\psi_{q'}^{e(g)}$. Simple selection rules follow if one has $k=N\pi/L$ with N a positive integer and $\phi=0$. Under these conditions one obtains couplings only between the single-atom wave functions

$$\cdots \leftrightarrow \psi_{2N-q}^{g/e} \leftrightarrow \psi_{N-q}^{e/g} \leftrightarrow \psi_q^{g/e} \leftrightarrow \psi_{q+N}^{e/g} \leftrightarrow \psi_{q+2N}^{g/e} \leftrightarrow \cdots \tag{11}$$

with $1 \leq q < N$. The coupling coefficients are all equal besides the one between ψ_{N-q} and ψ_q, which is of the same magnitude but of opposite sign. After suitable identifications the equations of motion for the probability amplitudes of the two-atom system can thus be cast into a form identical to Eqs. (7)–(9) apart from this sign peculiarity. An important special case in the coupling scheme of expression (11) arises if $q=N$. Under these circumstances the sequence terminates at ψ_q, the part to the left of it being obsolete. This special case is of particular importance in the discussion of exact dark states beyond the RNA.

III. NUMERICAL RESULTS

In order to set the stage for the two-atom problem, let us first take a brief look at its one-atom counterpart. With the help of the procedure used to derive Eqs. (7)–(9), we can obtain a similar set of equations for the one-atom system,

$$i\dot{C}_{1,m}=\omega_m C_{1,m}+\frac{g}{2}(C_{2,m+1}+C_{2,m-1}), \tag{12}$$

$$i\dot{C}_{2,m}=(\omega_m+\Delta-i\kappa/2)C_{2,m}+\frac{g}{2}(C_{1,m+1}+C_{1,m-1}), \tag{13}$$

where the notations used here are defined in parallel to those for the two-atom case. In particular, we now have $\omega_m=(q_0+m\hbar k)^2/(2\hbar M)$. The excited and ground state amplitudes are denoted C_1 and C_2, respectively. Equations (12) and (13) are very similar in structure to those used in the discussion of near-resonant scattering of two-level atoms from a standing-wave laser field [14]. Physically, they describe the atomic momentum spread during the interaction with the cavity mode. If we imagine the standing-wave mode as being composed of two counterpropagating running waves, we see that during an emission-absorption cycle the atomic momentum

can change by an amount of 0 or $2\hbar k$. The change depends on whether the photon is emitted into and absorbed from the same running wave mode or not. Successive cycles thus lead to an atomic momentum spread, i.e., heating.

This is illustrated in Fig. 1, which shows momentum distributions $P_m(\tau)=|C_{1,m}(\tau)|^2+|C_{2,m}(\tau)|^2$ derived from Eqs. (12) and (13) as a function of the discrete momentum index m and the dimensionless time $\tau=\omega_{\text{rec}}t$, with $\omega_{\text{rec}}=\hbar k^2/(2M)$ being the recoil frequency. These distributions illustrate the effective Hamiltonian time evolution of the atom before the photon escapes the cavity, governed by the non-Hermitian Hamiltonian

$$H_{\text{eff}}=H_a+H_c+H_{ca}-i\hbar\frac{\kappa}{2}a_c^\dagger a_c, \tag{14}$$

H_a and H_{ca} referring now to a single two-level atom. The initial conditions for the wave function were chosen as $C_{1,m}=\delta_{m,0}$, $C_{2,m}=0$, and $q_0=0$. Figures 1(a) and 1(b) display the case of a lossless cavity ($\kappa=0$) and a dimensionless atom-cavity coupling constant $\Omega=g/2\omega_{\text{rec}}=50$. In Fig. 1(a), the influence of the kinetic energy term $\hat{p}^2/2M$ is neglected (the Raman-Nath approximation) and the momentum spread grows linearly in time at a rate proportional to $\Omega\tau$. This should be compared to Fig. 1(b), which is for the full model including the kinetic energy terms. This illustrates the well-known fact that the RNA is only valid for short enough times. Due to the increasing mismatch between the photon energy and the atomic energy increment accompanying a photon absorption, the width of the momentum distribution eventually stops growing and begins to oscillate. The effects of cavity damping are illustrated in Figs. 1(c) and 1(d), which again compare the momentum distributions in the RNA and the full model, but for a moderate cavity damping rate $\kappa'=\kappa/\omega_{\text{rec}}=20$, i.e., $\kappa'/\Omega=0.4$. In this case the excited-state population is damped on a time scale approximately given by $4/\kappa'$.[1]

We now turn to the two-atom situation, with the goal of determining how the previous results are modified when we insert a second atom into the cavity. The dramatic changes brought about under these circumstances are illustrated in Figs. 2(a)–2(d), which show results of the numerical integration of Eqs. (7)–(9). They depict the momentum distribution of the first atom before the photon escape, $P_m^{(1)}(\tau)=\Sigma_{i=1,2,3;n}|C_{i,m,n}(\tau)|^2$, as a function of m and τ in both the RNA and the full model, and in the absence or presence of cavity losses. The initial conditions were chosen such that both atoms are at rest but atom 1 is in the excited state, atom 2 is in the ground state, and no photon is present in either the cavity or the vacuum modes, i.e.,

$$C_{i,m,n}(t=0)=\delta_{i,1}\delta_{m,0}\delta_{n,0} \tag{15}$$

---

[1]It should be noted that for large cavity damping $\kappa'\gg\Omega/2$ the decay rate of the excited state population goes to zero. This stabilization effect, however, is different in nature from the two-atom dark states discussed below.
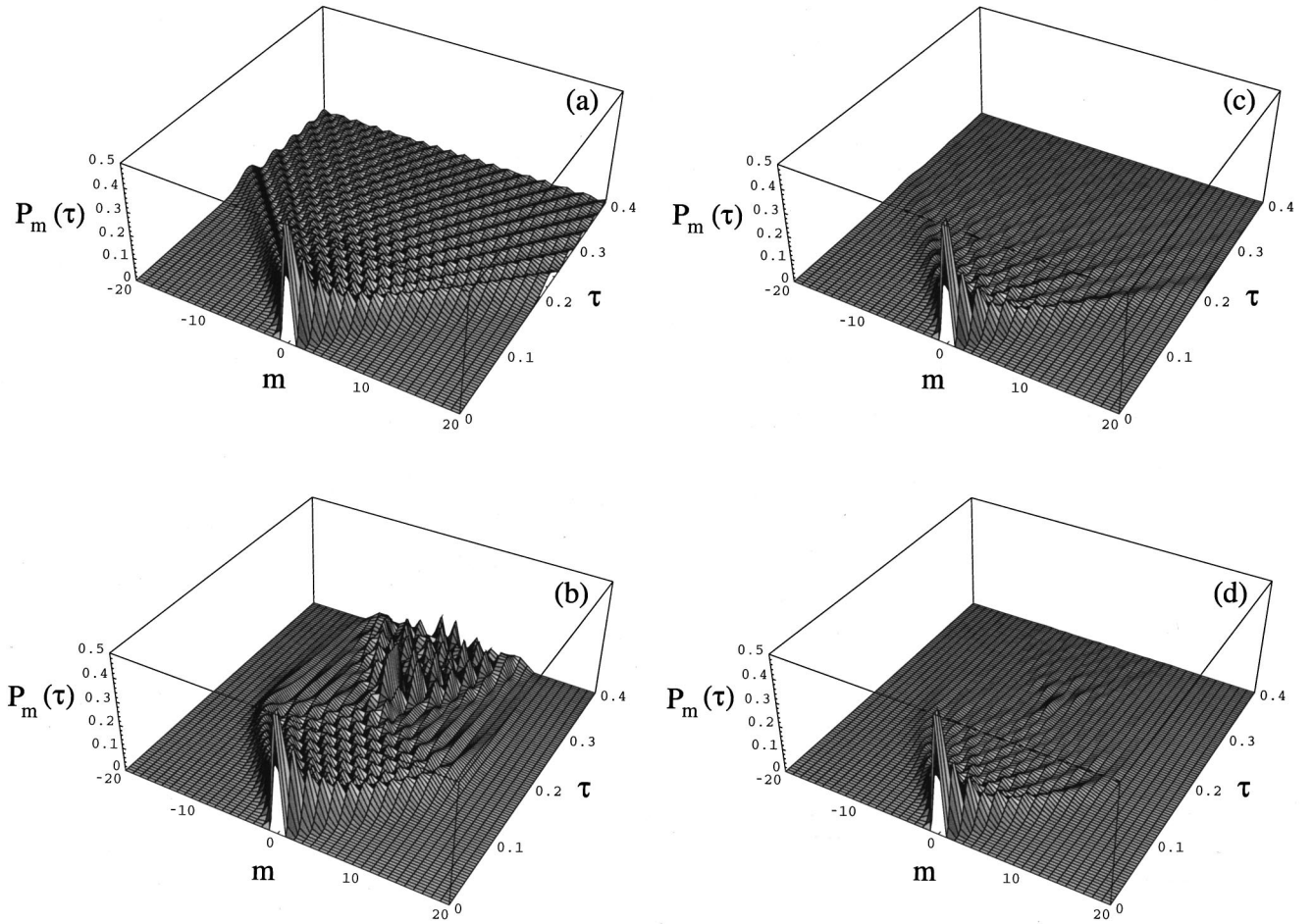
FIG. 1. Time evolution of the single-atom momentum distribution P_m for parameter values $\Delta=0$, $\Omega=50$. Initially, the atom is at rest in the excited state, and no photons are in the cavity and the vacuum. (a) RNA and $\kappa'=0$, (b) full model and $\kappa'=0$, (c) RNA but $\kappa'=20$, (d) full model and $\kappa'=20$.

and $p_{01}=p_{02}=0$. The atom-cavity coupling is again set to $\Omega=50$. As a consequence of the selection rules mentioned in Sec. II, one has for these initial conditions

$$P_m^{(1)}=\sum_n |C_{1,m,n}|^2$$

for m even and

$$P_m^{(1)}=\sum_n |C_{2,m,n}|^2+|C_{3,m,n}|^2$$

for m odd. Figures 2(a) and 2(b) display the case of the lossless cavity. One can recognize two main qualitative differences from the corresponding Figs. 1(a) and 1(b). First, the momentum distribution no longer spreads significantly: rather, it remains concentrated in the central mode (i.e., $m=0$) and a small number of side modes. The other modes remain almost unpopulated. Second, the comparison between the RNA and the full model results shows that the influence of the kinetic energy terms now is much smaller than in the one-atom case. Contrary to Figs. 1(a) and 1(b), for the time considered they only lead to some quantitative modifications but not to a qualitative change. This property is of course due to the concentration of the momentum distribution around

$m=0$. It also indicates that the RNA is a valuable tool in the interpretation of the two-atom behavior.

The study of the momentum distribution in the presence of cavity losses [Figs. 2(c) and 2(d), again with $\kappa'=20$] also yields a surprising result. One finds again that only a small number of modes are significantly populated. But in addition, and in contrast to the one-atom case, after an initial transient evolution the total atomic population decays only very slowly, i.e., *the photon escape from the cavity is strongly inhibited by the presence of a second atom.* In fact, the time evolution of the distribution still bears a strong similarity to the lossless case. Furthermore, the RNA yields a good approximation to the full model also in the presence of losses. A further increase of the cavity damping rate only leads to minor changes in the behavior of the momentum distribution.

A closer look at the long-time behavior is provided in Fig. 3. There, the total probability $P=\sum_m P_m^{(1)}$ of finding the excitation in the cavity (curve 1) is shown for the RNA (a) and the full model (b). The parameter values are chosen as in Figs. 2(c) and 2(d). After a rapid initial transient, the probability P reaches a constant value in the RNA, whereas it still decays slowly in the full model. The curves 2 and 3 show the time evolution of $|C_{1,0,0}|^2+|C_{1,0,\pm2}|^2+|C_{1,\pm2,0}|^2$ $+|C_{2,\pm1,\pm1}|^2$ (i.e., the central and the most highly populated
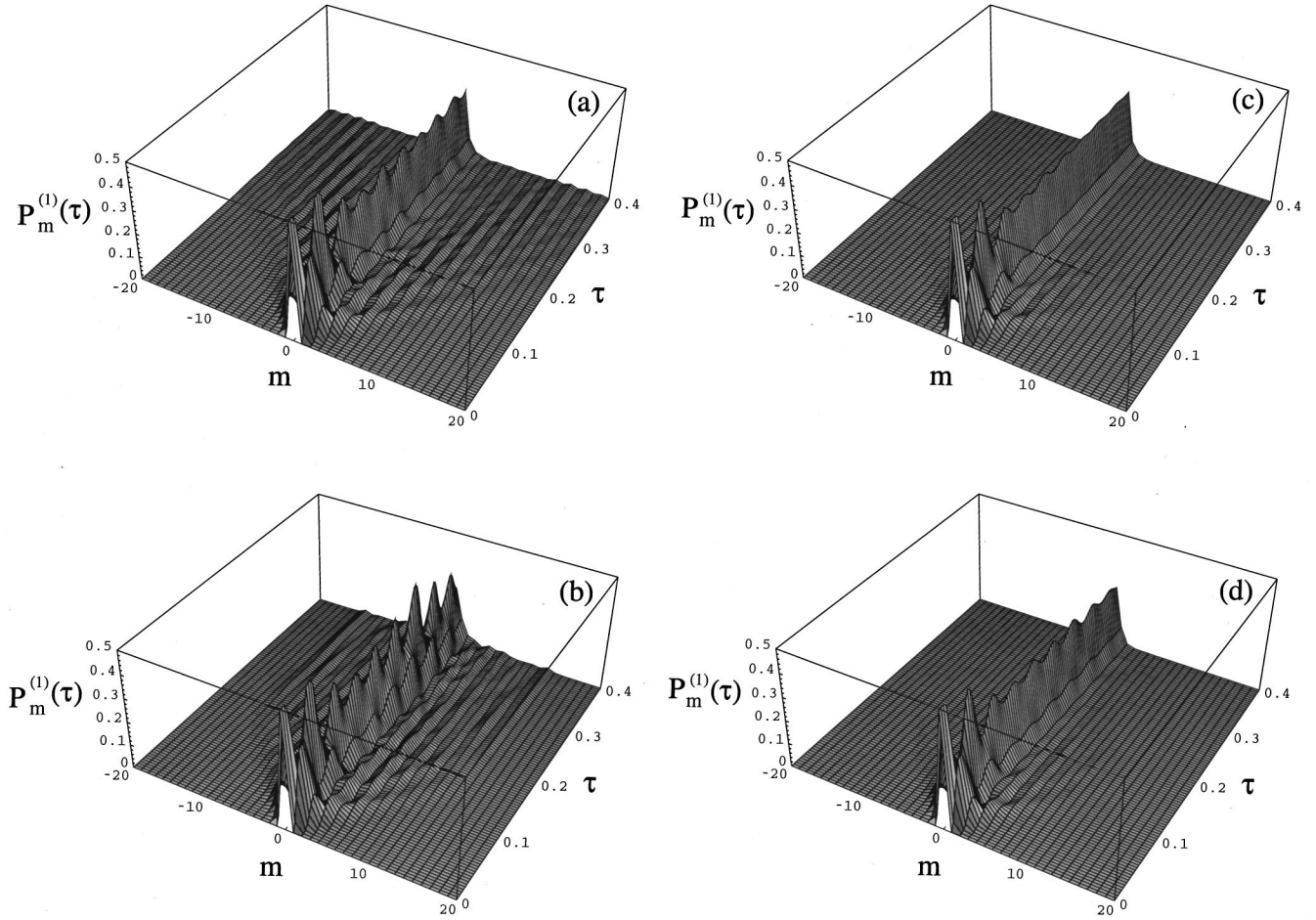
FIG. 2. Time evolution of the momentum distribution $P_m^{(1)}$ for the first atom in the two-atom problem. Initially, both atoms are at rest and atom 1 is excited; no photons are in the cavity and the vacuum. Parameter values and use of RNA for (a)–(d) are the same as in Fig. 1.

side modes) and of $|C_{1,0,0}|^2$ alone, respectively. These curves again demonstrate that the spread in momentum is strongly suppressed.

IV. TWO-ATOM DARK STATES

The results of Figs. 2 and 3 indicate that the atomic time evolution is characterized by the appearance of dark states which have the initial excitation stored in the atoms and which are almost immune to cavity damping. In this section a detailed analysis of these dark states is given. Before turning to the full problem, we first work in the RNA, which was shown to provide a useful approximate description.

A. Two-atom dark states in the Raman-Nath approximation

In order to investigate the dark states, it is convenient to work also in the position-space representation. The equations of motion for the position-dependent probability amplitudes $C_i(x_1,x_2,t)$ read

$$i\dot{C}_1 = -\frac{\hbar}{2M}\left(\frac{\partial^2}{\partial x_1^2}+\frac{\partial^2}{\partial x_2^2}\right)C_1 + g\cos(kx_1)C_3, \quad (16)$$

$$i\dot{C}_2 = -\frac{\hbar}{2M}\left(\frac{\partial^2}{\partial x_1^2}+\frac{\partial^2}{\partial x_2^2}\right)C_2 + g\cos(kx_2)C_3, \quad (17)$$

$$i\dot{C}_3 = \left[-\frac{\hbar}{2M}\left(\frac{\partial^2}{\partial x_1^2}+\frac{\partial^2}{\partial x_2^2}\right)+\Delta-i\kappa/2\right]C_3$$
$$+ g[\cos(kx_1)C_1+\cos(kx_2)C_2]. \quad (18)$$

In the first special case discussed in Sec. II (i.e., the atomic wave packet well localized inside the trap) these equations have to be solved in the domain $0 \leq x_1, x_2 \leq 2\pi/k$ and the solution must be of the form

$$C_i = \exp(ip_{01}x_1+ip_{02}x_2)\tilde{C}_i \quad (19)$$

with $\tilde{C}_i$ fulfilling periodic boundary conditions. In the second case (trap conditions taken fully into account) one has to consider solutions with vanishing Dirichlet boundary conditions in the domain $0 \leq x_1, x_2 \leq L$.

In the RNA, i.e., after discarding the spatial derivatives, Eqs. (16)–(18) decouple spatially and can be solved immediately. At a given point (x_1, x_2) they form a homogeneous linear 3×3 system of ordinary differential equations the eigenvalues of which are given by
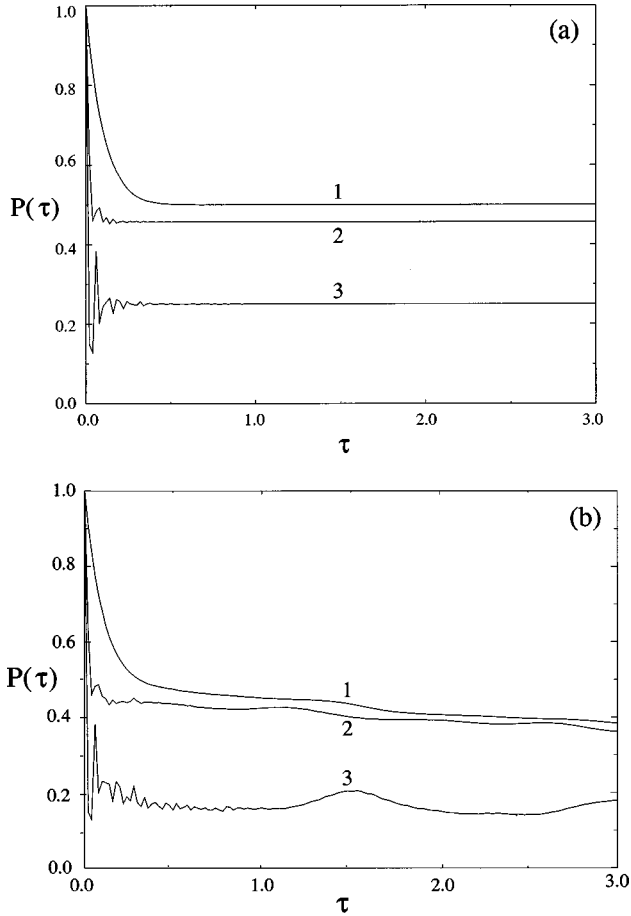
$$\lambda_1 = 0, \quad (20)$$

FIG. 3. Time evolution of the total probability $P(\tau)$ to find the excitation in the cavity (curve 1), of $|C_{1,0,0}|^2+|C_{1,0,\pm2}|^2+|C_{1,\pm2,0}|^2+|C_{2,\pm1,\pm1}|^2$ (curve 2), i.e., the central mode and the most highly populated side modes, and of $|C_{1,0,0}|^2$ alone (curve 3). The parameter values are $\Delta=0$, $\Omega=50$, $\kappa'=20$. (a) RNA, (b) full model.

$$\lambda_{2,3}=-\kappa/4-i\Delta/2$$
$$\pm\sqrt{\left(\frac{\kappa}{4}+i\frac{\Delta}{2}\right)^2-g^2[\cos^2(kx_1)+\cos^2(kx_2)]}.$$

$$(21)$$

The existence of the eigenvalue λ_1 whose real part vanishes independently of the values of x_1, x_2, and κ ensures that an excitation initially present in the system has a finite probability of remaining in it in the limit $t\to\infty$. In particular, if the atomic wave function is given at time $t=0$ by

$$|\psi(x_1,x_2,0)\rangle=A_1(x_1,x_2)|e,g,0,\{0_\mu\}\rangle$$
$$+A_2(x_1,x_2)|g,e,0,\{0_\mu\}\rangle$$
$$+A_3(x_1,x_2)|g,g,1,\{0_\mu\}\rangle,\qquad(22)$$

then the asymptotic state reached by the "atoms + cavity mode" system is characterized by the probability amplitudes (arranged as a column vector in a self-evident way)

$$[\cos^2(kx_1)+\cos^2(kx_2)]^{-1}$$
$$\times\begin{pmatrix} A_1\cos^2(kx_2)-A_2\cos(kx_1)\cos(kx_2) \\ -A_1\cos(kx_1)\cos(kx_2)+A_2\cos^2(kx_2) \\ 0 \end{pmatrix}.$$

$$(23)$$

Note that this state is *not* normalized, a result of the fact that some of the initial excitation has irreversibly escaped from the cavity into the reservoir.

Expression (23) shows that the asymptotic state does not have a contribution from the initial amplitude A_3, and furthermore the final amplitude in the third channel where the photon is present in the cavity vanishes. On the other hand, if a state has nonvanishing contributions A_1 or A_2 it will always evolve into a dark state unless $A_1\cos(kx_2)=A_2\cos(kx_1)$. The time scale to reach the dark state is determined by the eigenvalues λ_2 and λ_3.

From Eqs. (16)–(18) or Eq. (23) it follows that a given state is a dark state if and only if it is of the form

$$A(x_1,x_2)\begin{pmatrix} \cos(kx_2) \\ -\cos(kx_1) \\ 0 \end{pmatrix}$$

$$(24)$$

and, in addition, it fulfills the appropriate boundary conditions. The state (24) can be viewed as a generalization of the dark state in the Dicke theory of subradiance and superradiance [13].

In the following discussion we concentrate on the case of localized atoms in the sense of Sec. II. If one substitutes for the function A of expression (24) the set of plane waves $\exp(iq_{01}x_1+iq_{02}x_2)\exp[imkx_1+i(n+1)kx_2]$, one obtains a family of dark states $\{|d_{mn}\rangle\}$ which have a simple structure in momentum space, i.e.,

$$|d_{mn}\rangle=\tfrac{1}{2}[|(e,m),(g,n)\rangle+|(e,m),(g,n+2)\rangle$$
$$-|(g,m+1),(e,n+1)\rangle-|(g,m-1),(e,n+1)\rangle],$$

$$(25)$$

where we have omitted the occupation numbers of the photon modes in the notation of the ket vectors for simplicity. The dark states $|d_{mn}\rangle$ are truly entangled states. Since all permissible functions A can be expanded onto the indicated set of plane waves, the family $\{|d_{mn}\rangle\}$ forms a basis of the "dark" subspace of the total Hilbert space. However, this is not an orthogonal basis as a given $|d_{mn}\rangle$ has a nonvanishing scalar product with four other $|d_{m'n'}\rangle$.

Of particular interest in our context is the question of how to characterize the asymptotic state $|D_{mn}^{e/g,g/e}\rangle$ associated with a given initial state $|(e/g,m),(g/e,n)\rangle$. Its coordinate representation can be inferred immediately from Eq. (23), but further insight into the nature of the state can be obtained from its momentum distribution. Equations (7)–(9) show that it is sufficient to study this question for the state $|D_{00}^{eg}\rangle$, since the distributions for the other states can be obtained by a suitable shift of indices. In coordinate space the state $|D_{00}^{eg}\rangle$ is represented by

$$[\cos^2(kx_1)+\cos^2(kx_2)]^{-1}$$

$$\times(\cos^2(kx_2),-\cos(kx_1)\cos(kx_2),0)^T. \quad (26)$$

Its momentum-space amplitudes

$$c_{1/2,m,n}=\langle(e/g,m),(g/e,n)|D_{00}^{eg}\rangle$$

are determined by

$$c_{i,m,n}=\frac{k}{2\pi}\int\int_0^{2\pi/k}dx_1dx_2\,e^{-i(mkx_1+nkx_2)}$$

$$\times\frac{f_i(x_1,x_2)}{\cos^2(kx_1)+\cos^2(kx_2)} \quad (27)$$

with $f_1=\cos^2(kx_2)$ and $f_2=-\cos(kx_1)\cos(kx_2)$. As discussed in Sec. II, $c_{1(2),m,n}\neq0$ only for m,n both even (odd). Evaluating the integrals (27) one finds that the amplitudes $c_{1,2m,0}$, $m\geq0$, are given by

$$c_{1,2m,0}=\delta_{m,0}+\frac{i}{2\pi}(I_m+I_{m-1}), \quad (28)$$

where the numbers I_m satisfy the recurrence relation

$$I_m=\frac{1}{m}[(-1)^{m-1}4i-(6m-3)I_{m-1}-(m-1)I_{m-2}] \quad (29)$$

and $I_0=I_{-1}=i\pi/2$. Further relations between the amplitudes $c_{i,m,n}$ are given by

$$c_{1,m,n}+c_{1,m+2,n}+c_{2,m+1,n+1}+c_{2,m+1,n-1}=0, \quad (30)$$

$$c_{1,m,n}+c_{1,m,n+2}-c_{2,m+1,n+1}-c_{2,m-1,n+1}$$
$$=\delta_{m,0}(\delta_{n,0}+\delta_{n,-2}), \quad (31)$$

$$c_{i,m,n}=c_{i,\pm m,\pm n} \quad (32)$$

with m,n both even in Eqs. (30) and (31). Equation (30) is a direct consequence of Eq. (9) whereas Eq. (31) follows from the relation

$$|d_{00}\rangle=(|D_{00}^{eg}\rangle+|D_{02}^{eg}\rangle-|D_{11}^{ge}\rangle-|D_{-1,1}^{ge}\rangle)/2.$$

With the help of Eqs. (28)–(32) all amplitudes $c_{i,m,n}$ can be calculated iteratively. In this way, one obtains, for example,

$$c_{1,0,0}=1/2,$$

$$c_{2,\pm1,\pm1}=1/\pi-1/2\approx-0.1817,$$

$$c_{1,\pm2,0}=-c_{1,0,\pm2}=1/2-2/\pi\approx-0.1366.$$

An interesting way to determine the scalar products $\langle D_{m,n}^\sigma|D_{00}^{eg}\rangle$ with $\sigma=eg$ or ge proceeds as follows [the method can also be used to derive Eq. (31)]. The asymptotic state $|D_{00}^{eg}\rangle$ into which $|(e,0),(g,0)\rangle$ evolves is uniquely determined. Any state in the ''dark subspace'' orthogonal to $|D_{00}^{eg}\rangle$ must have vanishing overlap with $|(e,0),(g,0)\rangle$. If we denote by $|\bar{D}_{00}^{eg}\rangle$ the state $|D_{00}^{eg}\rangle$ after normalization—

remember that the dark state into which a given initial state evolves is not normalized—we must have that

$$|D_{00}^{eg}\rangle=|\bar{D}_{00}^{eg}\rangle\langle\bar{D}_{00}^{eg}|(e,0),(g,0)\rangle.$$

Comparing coefficients one obtains that

$$\langle D_{00}^{eg}|D_{00}^{eg}\rangle=0.5, \quad (33)$$

i.e., the system has a 50% probability to be trapped in that dark state. Using the Gram-Schmidt orthogonalization scheme to construct from $|D_{m,n}^\sigma\rangle$ a state orthogonal to $|\bar{D}_{00}^{eg}\rangle$ leads to the conclusion that

$$\langle D_{m,n}^\sigma|D_{00}^{eg}\rangle=c_{k,m,n} \quad (34)$$

with $k=1(2)$ if $\sigma=eg(ge)$, i.e., the asymptotic dark states are nonorthogonal, in general. Equations (33) and (34) can be verified by evaluating the scalar product in position space.

From Eqs. (28)–(33) it can be inferred that 50% of the population of the dark state is trapped in the state $|(e,0),(g,0)\rangle$, while the states $|(i,m),(j,n)\rangle$ with $|m|+|n|\leq2$ (4) hold 91.3% (96.3%) of the population. This observation explains the localization of the momentum distributions in Figs. 2 and 3.

B. Exact and approximate dark states in the full model

Turning to the full model described by Eqs. (7)–(9) or Eqs. (16)–(18), i.e., taking the kinetic energy terms into account, it becomes apparent that, in general, the states $|d_{mn}\rangle$ and $|D_{mn}\rangle$ are no longer exactly dark. By ''exactly dark'' we mean being an eigenstate of the full Hamiltonian with a purely real eigenvalue. It is therefore natural to ask whether the full model sustains exact dark states at all. Interestingly, a complete answer to this question can be given for both cases discussed in Sec. II, i.e., for atoms localized well inside the trap and for atoms experiencing the trap boundaries. In the first situation there are precisely two exact dark states, which are given by

$$|D_1\rangle=|d_{0,-1}\rangle=(\cos(kx_2),-\cos(kx_1),0)^T \quad (35)$$

and

$$|D_2\rangle=\sin(kx_1)\sin(kx_2)(\cos(kx_2),-\cos(kx_1),0)^T$$
$$=|d_{-1,0}\rangle-|d_{1,0}\rangle+|d_{1,-2}\rangle-|d_{-1,-2}\rangle. \quad (36)$$

Dark states thus appear only if the atomic momenta involved are integer multiples of $\hbar k$, i.e., if $q_{01}=q_{02}=0$. For the second case, in which the atomic wave functions extend over the whole length of the trap, it can be shown that exact dark states can only exist if in the cavity mode function of Eq. (4) $k=\pi N/L$ with integer $N\geq1$ and $\phi=0$. Under these conditions there is precisely one such state which, in the coordinate representation, is given by the first line of Eq. (36).

For proof of uniqueness of these dark states one can start from the observation that also in the full model exact dark states have to be of the form (24). Additionally, they now also must be eigenfunctions of $(\hat{p}_1^2+\hat{p}_2^2)/2M$ under the appropriate boundary conditions. One then expands both $A(x_1,x_2)$ and $A(x_1,x_2)\cos(kx_{1/2})$ onto a suitable set of

eigenfunctions. The fact that in the expansion of $A(x_1,x_2)\cos(kx_{1/2})$ there should only appear terms of the same energy imposes severe restrictions on the possible forms for the expansion of $A(x_1,x_2)$. These requirements can only be met in the cases indicated. For the situation in which the atoms extend over the whole trap, the breakoff of the coupling scheme (11) if $q=N$ (as outlined at the end of Sec. II) turns out to be crucial for the existence of the dark state.

These considerations imply that most dark states found in the RNA become unstable in the full model since they are orthogonal to the exact dark states, in general. The numerical results of Sec. III suggest, however, that the corresponding lifetimes are still very long so that these states may be regarded as ''quasidark.'' The examples shown referred to cases in which $\Omega,\kappa' \gg 1$, which is the relevant situation in practice as discussed in Sec. V. Under these conditions one may treat the kinetic energy term $(\hat{p}_1^2+\hat{p}_2^2)/2M$ as a small perturbation to the RNA Hamiltonian. Applying standard perturbation theory, one obtains an imaginary correction to the RNA dark state eigenenergies only in second order, which already indicates that these states will be long-lived. A crude estimate of the second-order imaginary part shows that the state $|D(d)_{mn}\rangle$ acquires a finite decay rate that is of the order of

$$\Gamma_{mn} \simeq \omega_{\text{rec}}(\tilde{m}^2+\tilde{n}^2)^2 \kappa'/\Omega^2. \tag{37}$$

Thereby, $\tilde{m}$ and $\tilde{n}$ have to be understood as typical values of m and n appearing in the expansion into center-of-mass momentum states. The estimate (37) assumes that κ' is not too large in comparison to Ω so that the square root in expression (21) is essentially imaginary.

Hence, consistent with the numerical calculations, we find that the lifetime of the ''quasidark states'' is long compared to ω_{rec}^{-1} under the condition $\Omega,\kappa' \gg 1$. Furthermore, our estimate implies that the decay rate increases rapidly for increasing m,n. This is as can be expected, since under these circumstances the dephasing between the different momentum eigenstates becomes faster. The dependence on κ' and Ω suggests that the coupling to the decay channel becomes more efficient when κ' is increased and Ω decreased. Figure 4 shows the decay of the dark states $|d_{mn}\rangle$ for various values of (m,n), κ', and Ω. Their evolution qualitatively confirms the dependence (37) of Γ_{mn} on these parameters. Thereby, curve (a) should be compared to curves (b), (c), and (d) as in each one of these one relevant parameter is changed in comparison to (a).

V. SUMMARY AND CONCLUSIONS

In this paper we have investigated the dynamics of two two-level atoms coupled to a single damped mode of an electromagnetic resonator, including the effects of photon recoil. We concentrated on the situation where one quantum of excitation is initially present in the system. A generic feature of the atomic evolution is the appearance of dark states. These states, in which the excitation is stored in the internal atomic degrees of freedom, are almost immune to photon decay from the cavity. When in a dark state, the two atoms become quantum mechanically entangled and form a
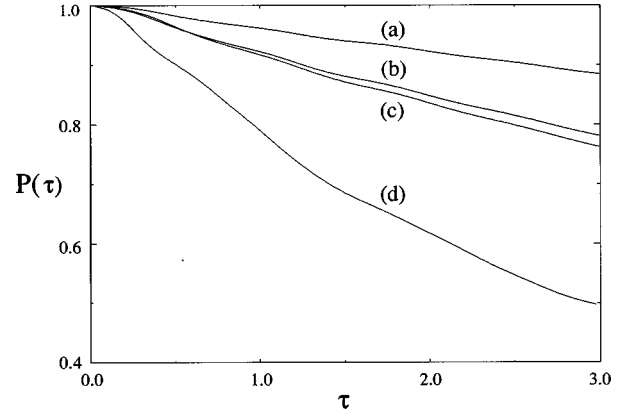

FIG. 4. Total survival probability $P(\tau)$ for initial states $|d_{mn}\rangle$ in the full model under various conditions. Parameter values (a) $m=n=0$, $\kappa'=20$, $\Omega=50$; (b) $m=n=0$, $\kappa'=100$, $\Omega=50$; (c) $m=n=0$, $\kappa'=20$, $\Omega=25$; (d) $m=0$, $n=2$, $\kappa'=20$, $\Omega=50$.

new kind of ''molecule'' bound by the quantum of excitation that they share. The state of the compound system can conveniently be described in terms of a superposition of different states of well-defined center-of-mass momentum. A remarkable characteristic feature of the dark states is their small momentum spread, as compared, e.g., to the one-atom situation. This property makes their description in the Raman-Nath approximation quite accurate. While most dark states become only ''quasidark'' when this approximation is removed, their damping rate remains quite long indeed.

When considering the possible practical realization of these states, an interesting question concerns the influence of a nonconstant atomic trapping potential on the time evolution of the dark states. If the trapping potentials can be arranged to be equal for ground and excited states, then one can still obtain dark states in the RNA (for the full model it can be anticipated that exact dark states will not exist any longer, in general). If, as is normally the case, these potentials differ from each other, even the RNA will not support dark states. However, as Eqs. (16)–(18) show, in the vicinity of the line $x_1=x_2$ the decay will be significantly decelerated so that a remnant of the dark-state effect might still be visible under such circumstances.

Let us conclude with a brief discussion of the experimental feasibility to observe such two-atom dark states. Recent cavity QED experiments in the microwave and optical domain are described, e.g., in Refs. [5,15,16]. They typically involve a low-density atomic beam passed through the electromagnetic resonator, a situation that can be modeled in terms of the localized wave packet description of Sec. II. In these experiments the residual spontaneous atomic decay rate γ in the cavity (due to coupling to vacuum modes) is approximately one order of magnitude smaller than the cavity Rabi frequency g and damping rate κ, which are both comparable in magnitude. A single-mode description is thus adequate and our system (once prepared in the initial state) would have enough time to coherently evolve into a dark state. Furthermore, the recoil frequency ω_{rec} is also very small in comparison to g and κ (typically less than a factor of 10^{-3}) so the RNA should provide a very accurate description. In an experimental realization a main difficulty would certainly consist in efficiently preparing the initial system

state. From this point of view, the optical regime does not appear as promising as the microwave regime: First, due to the short free-space spontaneous lifetime of optical transitions, the atoms probably could not be prepared in the excited state before they enter the cavity. Second, if they are both simultaneously excited inside the cavity, the probability of coupling to the dark state is relatively low.

An experiment involving a microwave cavity might proceed as follows. Diatomic molecules in a low-intensity beam are dissociated such that the two fragments are of nonvanishing opposite spin. The atoms can thus be separated in an inhomogeneous magnetic field. One atomic beam is subsequently prepared in the Rydberg ground state, the other one in the excited state. Using atom optical elements, the two beams are guided such that they intersect each other in the microwave cavity (at a small angle). As the molecular dissociation creates atom pairs, it should be possible to arrange the setup so that both partners pass the cavity simultaneously with high probability. The experimental parameters should be chosen such that a single atom always leaves the cavity in the ground state. The signature of the formation of a dark state would consist in detecting an appreciable fraction of atoms leaving the cavity in the excited state. In order to obtain more information about the nature of the dark state, one could, for example, additionally observe the spatial atomic density distribution.

Note added in proof. In a recent publication, M. B. Plenio, S. F. Huelga, A. Beige, and P. L. Knight, Phys. Rev. A **59**, 2468 (1999) discuss the closely related problem of a cavity-loss-induced generation of entangled states. However, their paper ignores the role of the atomic center-of-mass motion.

ACKNOWLEDGMENTS

[1] P. Meystre, in *Progress in Optics 30*, edited by E. Wolf (Elsevier, New York, 1992).

[2] S. Haroche, in *Fundamental Systems in Quantum Optics*, edited by J. Dalibard, J.-M. Raimond, and J. Zinn-Justin (North-Holland, Amsterdam, 1992).

[3] E. M. Purcell, Phys. Rev. **69**, 681 (1946).

[4] D. Kleppner, Phys. Rev. Lett. **47**, 233 (1981).

[5] M. Brune, F. Schmidt-Kaler, A. Maali, J. Dreyer, E. Hagley, J. M. Raimond, and S. Haroche, Phys. Rev. Lett. **76**, 1800 (1996).

[6] U. Eichmann, J. C. Bergquist, J. J. Bollinger, J. M. Gilligan, W. M. Itano, D. J. Wineland, and M. G. Raizen, Phys. Rev. Lett. **70**, 2359 (1993).

[7] R. G. DeVoe and R. G. Brewer, Phys. Rev. Lett. **76**, 2049 (1996).

[8] P. Kochan, H. J. Carmichael, P. R. Morrow, and M. G. Raizen, Phys. Rev. Lett. **75**, 45 (1995).

[9] G. M. Meyer and G. Yeoman, Phys. Rev. Lett. **79**, 2650 (1997).

[10] T. Rudolph and Z. Ficek, Phys. Rev. A **58**, 748 (1998).

[11] G. Yeoman and G. M. Meyer, Phys. Rev. A **58**, 2518 (1998).

[12] E. V. Goldstein and P. Meystre, Phys. Rev. A **56**, 5135 (1997).

[13] R. H. Dicke, Phys. Rev. **93**, 99 (1954).

[14] A. P. Kazantsev, G. I. Surdutovich, and V. P. Yakovlev, *Mechanical Action of Light on Atoms* (World Scientific, Singapore, 1990).

[15] S. L. Mielke, G. T. Foster, and L. A. Orozco, Phys. Rev. Lett. **80**, 3948 (1998).

[16] C. J. Hood, M. S. Chapman, T. W. Lynn, and H. J. Kimble, Phys. Rev. Lett. **80**, 4157 (1998).